Contract No:

This document was prepared in conjunction with work accomplished under Contract No. DE-AC09-08SR22470 with the U.S. Department of Energy (DOE) Office of Environmental Management (EM).

Disclaimer:

Characterization of Oxide Films on Aluminum Materials following Reactor Exposure and Wet Storage in the SRS L-Basin

L. Olson, C. Verst, A. d'Entremont, R. Fuentes, R. Sindelar

March 2019

SRNL-STI-2019-00058, Revision 0

DISCLAIMER

Printed in the United States of America

Prepared for
U.S. Department of Energy

SRNL-STI-2019-00058
Revision 0

Keywords: *Aluminum spent nuclear fuel, spent fuel storage, corrosion*

Retention: *Permanent*

Characterization of Oxide Films on Aluminum Materials following Reactor Exposure and Wet Storage in the SRS L-Basin

L. Olson
C. Verst
A. d'Entremont
R. Fuentes
R. Sindelar

March 2019

Prepared for the U.S. Department of Energy under contract number DE-AC09-08SR22470.

Savannah River National Laboratory™
OPERATED BY SAVANNAH RIVER NUCLEAR SOLUTIONS

REVIEWS AND APPROVALS

AUTHORS:

_____
Luke C. Olson, Materials Applications and Process Technology, SRNL Date

_____
Christopher Verst, Materials Applications and Process Technology, SRNL Date

_____
Anna L. d'Entremont, Energy Materials, SRNL Date

_____
Roderick E. Fuentes, Corrosion and Materials Performance, SRNL Date

_____
Robert L. Sindelar, Materials Science and Technology, SRNL Date

TECHNICAL REVIEW:

_____
Poh-Sang Lam, Corrosion and Materials Performance, SRNL Date

APPROVAL:

_____
Marissa M. Reigel, Manager Date
Materials Applications and Process Technology, SRNL

_____
David T. Herman, Nuclear Materials Management, SRNL Date

_____
Michael J. Connolly, Idaho National Laboratory Date

TABLE OF CONTENTS

LIST OF FIGURES

LIST OF ABBREVIATIONS

ASNF	Aluminum-Clad Spent Nuclear Fuel
BSD	Backscattered Electron Detection
EDS	Energy Dispersive Spectroscopy
LEU	Low-Enriched Uranium
MURR	Missouri University Research Reactor
ORR	Oak Ridge Research Reactor
SEM	Scanning Electron Microscopy
SRNL	Savannah River National Laboratory
SRS	Savannah River Site
USH	Universal Sleeve Housing
XRD	X-Ray Diffraction

1.0 Executive Summary

This report describes the characterization of oxide films on one cropped piece of 6061, one 6063, and one cropped piece that could have been either 6061 or 6063 aluminum-based alloy, stored wet for up to approximately 40 years in L-Basin on the Savannah River Site (SRS). One 6061 cropping was from a Missouri University Research Reactor (MURR) fuel element. The 6063 piece was from a cropping from a Universal Sleeve Housing (USH). The Mark-16B fuel assembly could have been either 6061 or 6063 based on design drawings. Both the Mark-16B and USH were used in SRS Production Reactors. Characterization of the as-received oxides includes the oxide morphology, thickness, structure, and chemical composition. The aim is to characterize the oxide layer on aluminum cladding and fuel components that have reactor service and long-term basin storage service.

The work in this report comprises results and information prepared under Task 6, Milestone 6.5 in Task Technical and Quality Assurance Plan SRNL-RP-2018-00610.

The results of the characterization include:

- X-Ray diffraction (XRD) analysis revealed both bayerite ($Al(OH)_3$) and boehmite (AlO(OH)) on the surface of the MURR and USH samples, and bayerite, boehmite, and gibbsite ($Al(OH)_3$) on the surface of the Mark-16B sample. The presence of the bayerite on the USH, which is believed to have operated close to 90°C, suggests that further oxide growth in wet storage needs to be accounted for, despite the apparent protectiveness of the 185 °C prefilms.
- Comparison of the ratios of boehmite and bayerite XRD peaks indicates the USH had the highest exposure temperatures with the most boehmite being formed, followed by the MURR. The Mark-16B had the least boehmite detected. Estimated sample histories based on reactor documentation supports these conclusions.
- Results of cross-section scanning electron microscopy (SEM) showed the MURR oxide thickness was ~5 to ~10 µm, and the Mark-16B oxide thickness was ~5 to ~15 µm. The USH oxide thickness was indiscernible in cross-section with the mounting method performed and SEM capabilities available (although it was detected in plan-view and by XRD).
- The surface oxide morphology from plan-view of the MURR sample appears blocky and dense, which is expected to be more protective than a porous film.
- The surface oxide morphology from plan-view of the USH appeared globular and dense, which is expected to be more protective than a porous film.
- The surface oxide morphology from plan-view of the Mark-16B primary oxide appeared blocky but porous. When the thick oxide fractured off near the edges of the sample from cutting, it appeared a uniform thin oxide was present.

2.0 Introduction

2.1 Motivation for Sampling Oxyhydroxides on L-Basin Fuel Croppings

It is important to characterize the oxides observed on actual Aluminum-Clad Spent Nuclear Fuel (ASNF) cladding in both structure and composition to inform tasks associated with ASNF disposal. The oxides can be a source of hydrogen through radiolysis as well as water through adsorption, both of which may be functions of surface area. Therefore, the motivation for oxyhydroxide sampling on actual ASNF is to identify and characterize (quantify) oxyhydroxides present on ASNF cladding.

2.2 Cropping Operation and Storage Histories and Retrieval from L-Basin

Table 1 summarizes the croppings' estimated operation and storage minimum temperature and time histories, based on review of documentation on the reactors and storage basins.

Table 1 Estimated cropping in-reactor operation and post-discharge basin storage history.

Cropping	Minimum Operation Temperature (Celsius)	Operation Time (days)	Storage Temperature (Celsius)	Storage Time (years)
MURR	60	113	22.3**	<18
USH	37.8*	~1800	22.3**	~40
Mark-16B	37.8	~220	22.3**	~40

*The cropping is likely from an active fuel region and therefore its temperature may have been as high as the maximum outlet temperature of 93.3 ℃.[1]
**Average L-Basin temperature from 12/1992-12/2018.

The impact of corrosion during wet storage should also be considered. L-Basin temperature and chemistry have been actively monitored throughout its history. During the 1970's and early 1980's, water conductivity was maintained in the 60-70 µS/cm range.[2] Changes in pool chemistry associated with L-reactor mothballing and shutdown led to higher conductivity conditions, with conductivity ranging between 90-120 µS/cm during the 1987-1991 period, with a peak in 1991 reaching ~160 µS/cm.[2] The higher conductivity during this period was largely attributable to storage conditions where dissimilar metals were in contact, leading to galvanic corrosion. These conditions have since been remedied. Extensive deionization began in L-Basin in early 1994, and a series of deionizer systems were tested, bringing the conductivity down to near current values.[2] L-Basin chemistry has been recorded since ~12/1992, with temperature available since ~10/1996. Figure 1 and Table 2 summarize the L-Basin storage pool chemistry data from 12/1992-12/2018.

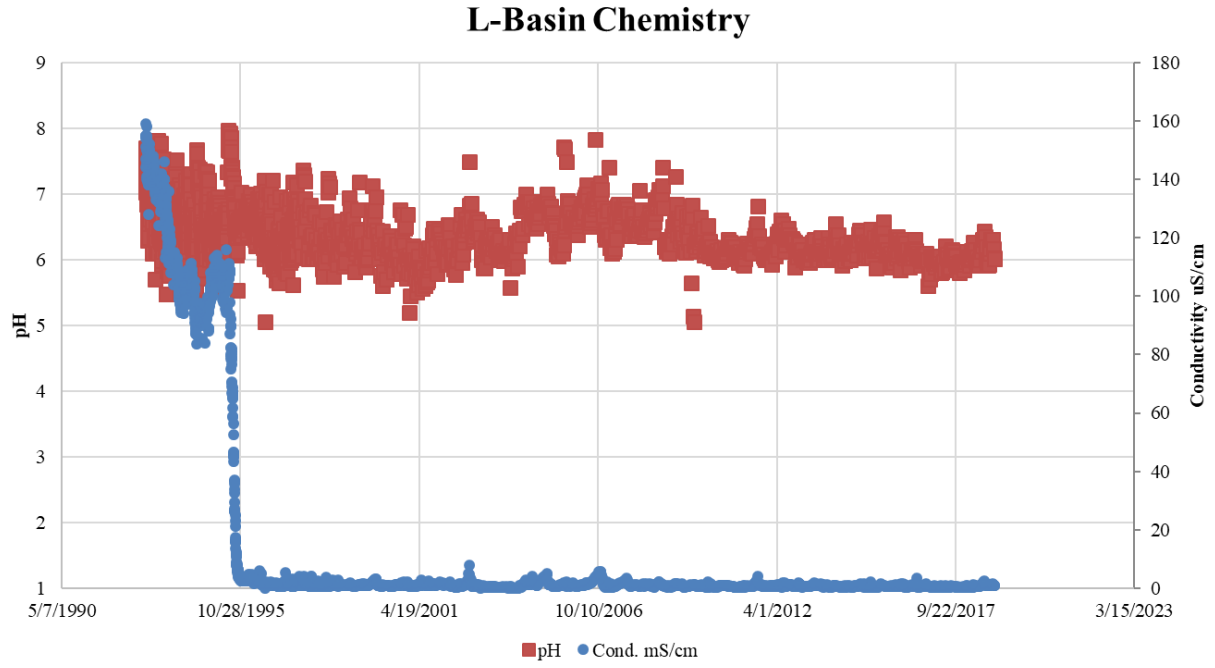

Figure 1 L-Basin wet storage pool pH and conductivity from 12/1992 to 12/2018.

Table 2 L-Basin storage pool temperature and chemistry 12/1992-12/2018

		12/1992–12/2018	
pH	Maximum	8.0	
	Minimum	5.1	
	Average	6.5	
		12/1992–12/1995	**01/1996–12/2018**
Conductivity (µS/cm)	Maximum	159.0	7.8
	Minimum	2.40	0.02
	Average	97.7	1.3
		10/1996–12/2018	
Temperature (°C)	Maximum	28.0	
	Minimum	14.6	
	Average	22.3	

Figure 2 shows the cropping pieces in their respective storage bins in L-Baisn prior to retreival for shipment to SRNL. One cropping each from a MURR fuel element, USH, and a Mark-16B assembly were collected (Figure 3, left), transferred underwater to a shipping cask on 8/22/2018 and 8/23/2018, and then shipped to A-area in late August 2018. Pieces were drip-dried on 8/29/2018 in the SRNL shielded cells facility.

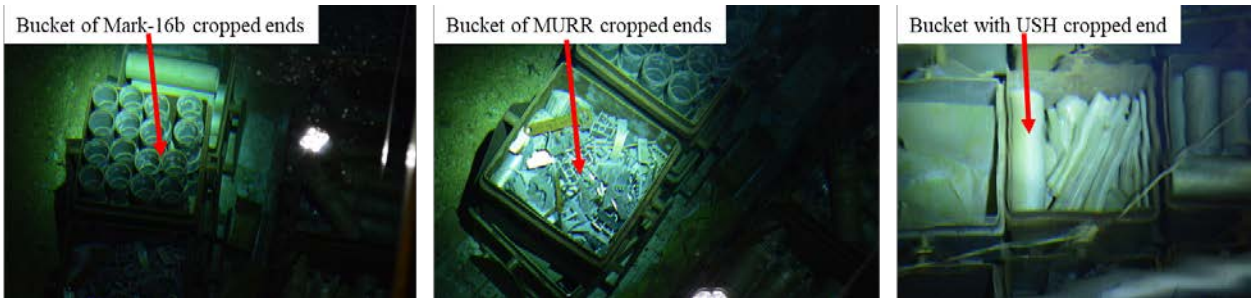

Figure 2 Scrap and croppings in wet storage in L-Basin.

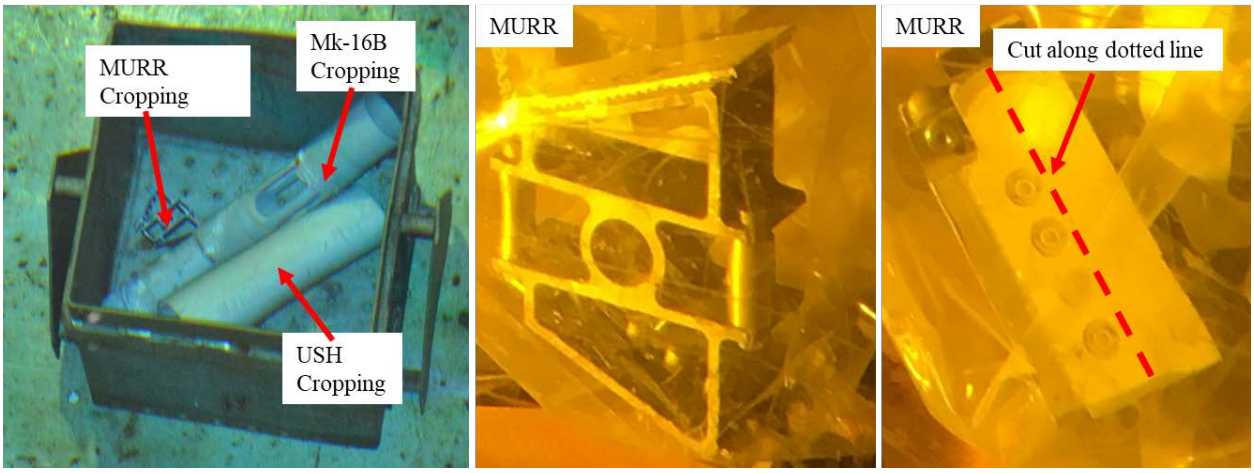

Figure 3 Left: L-Basin croppings to be analyzed. Middle and Right: MURR piece in shielded cells.

2.3 MURR Fuel Element Cropping Exposure and Storage History

The entire structure of the MURR fuel element was fabricated of Aluminum-Alloy 6061-T6 with stainless steel hardware.[3] The MURR has a well-documented reactor history and storage conditions. However, the MURR cropping was selected from a bucket of croppings (Figure 2, middle) and therefore fuel element-specific information was lost, such as which element it was from and whether the cropping was from the top or bottom of the element. This complicates determining a thermal history for the MURR sample. A minimum in-core temperature range, while operating under full power, can be estimated for the MURR cropping using operating parameters and core design knowledge. Note that passivation film evolution during non-operation times is unknown.

Figure 4 shows the MURR fuel element and core design [4]. Nearly all the coolant water runs past the plate fuel in the elements. Based on core coolant entry average temperatures of 60 °C, and exit of 70.7 °C from the license renewal application safety analysis report [3], it can be estimated that the cladding piece evaluated was at least 60 °C if it was from the inlet end of the element or 70.7 °C if it was near the exit. The temperatures may have been higher because the fuel elements generated power along their length and were in direct contact with the slotted aluminum side plate sampled. However, the high fuel-plate surface area and rapid drop off in power level as a function of distance from the center of the core could lessen this effect.[5]

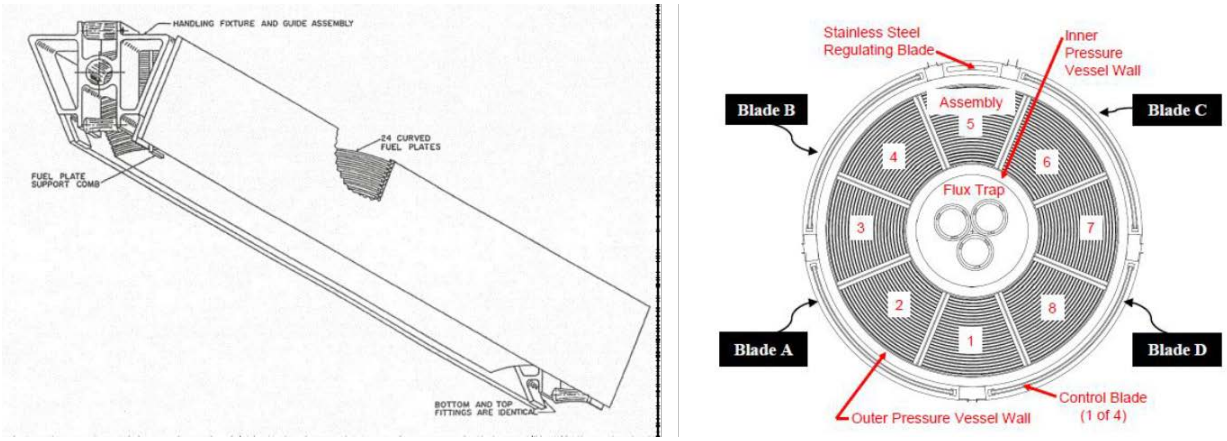

Figure 4 Left: MURR fuel element, Right: MURR Core design. Source: [4]

Table 3 Summary of MURR heat transfer data. Source: [3]

Parameter	5-MW Operation	10-MW Operation	Units
Average Power Density in Core	151	303	kW/liter
Average Specific Power	806.5	1613	kW/Kg ^{235}U
Reactor Core Coolant			
Total Flow Rate	1,800 (6,813)	3,600 (13,627)	gpm (lpm)
Design Inlet Temperature	140 (60)	140 (60)	°F (°C)
Estimated Pressure Drop Across the Fuel at 150°F (65.6 °C) Ave.	3.1 (21.4)	12.44 (85.8)	psi (kPa)
Min. Pressure at Vessel Inlet Nozzle	70.5 (486.1)	67.4 (464.7)	psia (kPa)
Min. Pressure at the Pressurizer	75.0 (517.1)	75.0 (517.1)	psia (kPa)
Heat Transfer Area	184.3 (17.1)		ft^2 (m^2)
Flow Area - Fuel Elements	0.3231 (0.0300)		ft^2 (m^2)
Total Flow Area	0.3505 (0.0326)		ft^2 (m^2)
Heat Fraction Released in Core	0.93		
Coolant Velocity in Core	11.55 (3.52)	23.10 (7.04)	ft/sec (m/sec)
Average Heat Flux	0.86×10^5	1.72×10^5	Btu/ft^2-h
Fuel Assembly Average Outlet Temp.	159.3 (70.7)	159.3 (70.7)	°F (°C)
Ave. Power Density in Hot Channel / Ave. Core Power Density	2.469*	2.469*	
Max. Power Density in Hot Channel / Ave. Power Density in Hot Channel	1.489*	1.489*	
Hot Spot Position on Fuel (Blades Half Out)	18 (45.7)	18 (45.7)	inches (cm)
Fractional Bulk Rise at Hot Spot	0.701	0.701	

*This value assumes worst-case - nonuniform core loading.

As of 2013, over 35 years of operation, the MURR averaged 6.3 days of operation each week, and discharged fuel elements after about 18–20 weeks of in-core operation.[5] Each element therefore operated in-core about 113-126 days at temperature. The 18-20 weeks of operation were non-sequential. All fuel elements were removed from the core every week and replaced with other elements that were either fresh or stored from previous runs, so that the core could start xenon-free each time.[5] A minimum temperature of 60 °C and a minimum time at temperature of 113 days can be assumed bounding. Furthermore, after each ~6.3 days of operation, there was no less than 7 days in wet storage. When out of the core, the fuel was stored in the main pool, which had a mixed bulk temperature of 37.8 °C.[3] Pool pH and conductivity data from 2018 can be viewed in Figure 5; other years are assumed to be similar.[6] In 2018, the maximum pool pH was 6.45; the minimum was 5.18, and the average was 5.77.[6] In 2018, the maximum pool conductivity was 2.72 mS/m; the minimum was 0.95 mS/m, and the average was 1.49 mS/m.[6] After final discharge from the reactor, the fuel was shipped to SRS L-Basin where it was put in a storage pool and cropped. The MURR cropping was moved to L-Basin no earlier than 2000, since prior to that offsite fuel was sent to the Receiving Basin for Offsite Fuel, and croppings were not moved from that facility when it was de-inventoried of used/spent fuel.[7]

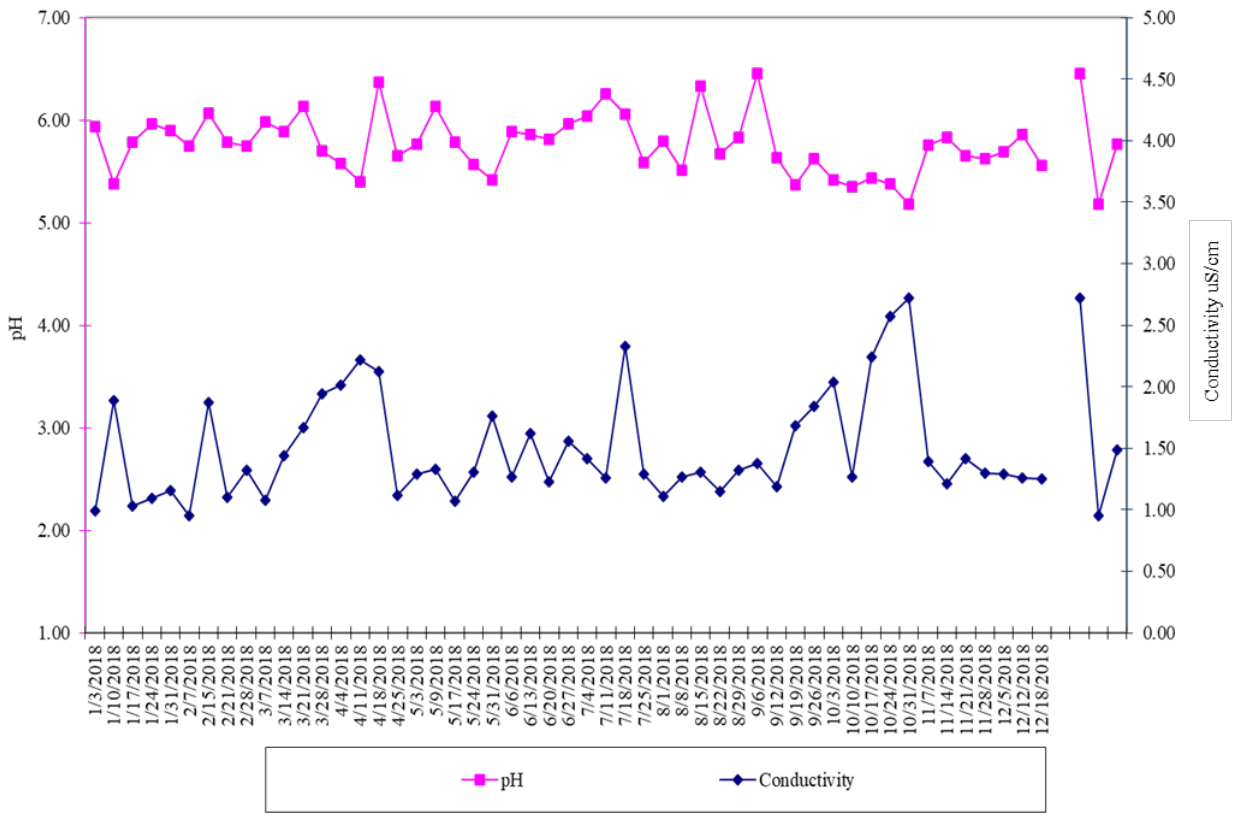

Figure 5 MURR pool pH and conductivity in 2018. Source: [6]

Due to the low power of the MURR (5-10 MW) and an estimated cladding temperature of around 60 °C – 70 °C during operation, this fuel is expected to have a thin oxide layer that is composed primarily of aluminum trihydroxide (gibbsite and/or bayerite), although it could also have boehmite if the temperature was high enough (e.g., due to proximity to the fuel dissipating heat).

2.4 USH Cropping Exposure and Storage History

The USH were made from aluminum alloy 6063 and used in the heavy-water production L-Reactor operated at SRS.[8, 9] While the USH were not deliberately pretreated to form a protective boehmite surface prior to operation, they did undergo flow testing which included steam drying, and the steam drying likely formed some boehmite on the surface.[7] The steam drying used superheated steam, lasted about 5 -10 minutes, although the exact superheated steam temperatures and times used could not be determined.[10] The USH cropping average exposure temperature was estimated from the process water system heat exchanger design data, obtained from Table 5.4-1 in the SRS Production Reactor Safety Analysis Report (SAR).[11] The process water heat exchanger had an average inlet temperature of 37.8 °C and an average outlet temperature of 93.3 °C.[11] The exact location of the USH cropping in relation to its placement in the core is unknown, so it could potentially have seen temperatures as low as 37.8 °C or as high as 93.3 °C. However, it is believed the USH croppings remaining in L-Basin are primarily from the active fuel length of the core, which is expected to be closer to the core outlet than inlet temperature.[12] The USHs were in core for about 5 years prior to replacement [13], after which they were stored wet in L-Basin since the 1970's.[1]

2.5 Mark-16B Cropping Exposure and Storage History

The Mark-16B cropping could have been from the P, K, or L heavy-water production reactors.[9] SRS drawings indicate the Mark-16B cropping was from the "auxiliary sleeve", and could have been fabricated using either 6061 (tempers T4, T6, T651, or T6511) or 6063 (tempers T4, T6, T651, or T6511).[14] While the Mark-16B assemblies were not deliberately pretreated to form a protective boehmite surface prior to operation, they did undergo flow testing which included steam drying similar to that performed on the USH, and the steam drying likely formed some boehmite on the surface.[7, 10] Indentations on the cropping and visible in SRS drawings indicate the cropping came from the top of the assembly[15], and SRS production reactors' coolant flowed from the top down [1], so the Mark-16B cropping probably saw temperatures of about 37.8 ℃. The Mark-16B assemblies were kept in core for ~7 months [13], after which they were stored wet since the 1970's.[1]

2.6 Literature Models

To orient expectations for the oxide thickness and morphology of the L-Basin croppings, a literature search was performed. It should be noted that the estimates made based on the literature search and correlations consider only in-core exposure, ignoring the potential oxide growth in the L-Basin storage pools subsequent to removal from operations, due to lack of data on oxide growth on top of a pre-existing oxide film.

2.6.1 Predictions for MURR oxide thickness based on exposure history

Relevant corrosion data for 6061 for similar exposure conditions could not readily be found to make predictions for the MURR fuel element cropping, however relevant data was found for Al-1100. Draley et al. [16] measured the corrosion of 1100 aluminum in oxygen-saturated water at 70 ℃ and 6.5 pH for up to 1.5 years, using two corrosion vessels. Each vessel tested contained multiple samples. The water in the first vessel was refreshed while the second received water from the first vessel (carrying corrosion products from the corrosion in the first vessel). It was found that the long-duration behavior was logarithmic, and the data was fitted in the form [16]

$$L = a \log_{10}\left(\frac{t}{1\ \text{day}}\right) + b$$

where L is mass of metal corroded per unit surface area in mg/dm^2, t is the exposure time in days, and a and b are fitted constants.

The expression to convert from the metal loss per area L to oxide thickness x_{ox}, assuming a dense and completely adherent film, is given by

$$x_{ox} = \frac{L}{M_{Al}} \frac{M_{ox}}{\rho_{ox}}$$

where $M_{Al} = 27\ \text{g/mol}$ and M_{ox} are the molar masses of Al metal and oxide and ρ_{ox} is the oxide density. For either trihydroxide, $Al(OH)_3$, the molar mass is $M_{ox} = 78\ \text{g/mol}$. The trihydroxide densities are slightly different: $\rho_{ox} = 2.42\ \text{g/cm}^3$ for gibbsite and $\rho_{ox} = 2.53\ \text{g/cm}^3$ for bayerite.[17]

The average fits reported and the corresponding predictions for metal loss and dense bayerite film thickness for the MURR are in Table 4. The reported fits differed significantly between the two vessels tested in reference [16] but were similar among specimens in the same vessel. The actual oxide film might be porous, which would tend to increase the thickness for a given mass of oxide. For MURR, the cumulative in-core exposure time averaged 18–20 cycles of 6.3 days in-core with at least 7 days in wet storage between cycles, i.e., an estimated 113–126 days in-core and an estimated 239-266 days total service life of alternating operation and wet storage. Estimates for 113 and 266 days are provided to bracket this window. Note that

the MURR cropping would have been exposed to forced coolant flow, while the Draley correlations were derived for minimal-flow conditions—the impact of water velocity on the oxide formation is uncertain.

Table 4 Literature model parameter values from reference [16] and calculated bayerite thickness for the MURR plate.

Vessel	a (mg/dm^2)	b (mg/dm^2)	$L(113\ days)$ (mg/dm^2)	$x_{ox}(113\ days)$ (μm)	$L(266\ days)$ (mg/dm^2)	$x_{ox}(266\ days)$ (μm)
1	3.23	35.59	42.2	4.8	43.4	5.0
2	2.78	30.20	35.9	4.1	36.9	4.2

2.6.2 Predictions for USH oxide thickness based on exposure history

Two correlations were found to estimate the oxide thickness on the USH, assuming it was exposed to near-outlet temperatures ~93°C. However, both correlations have been extrapolated far beyond the duration of the original data.

Using a similar set-up to reference [16] described above, Draley et al. [18], measured corrosion of Al-1100 over a shorter duration (45 days) at temperatures up to 95°C for O_2-saturated and He-saturated water. The measured corrosion was found to follow the same logarithmic form with different fitted constants. For boehmite, the expected oxide above 80°C, the molar mass is $M_{ox} = 60\ g/mol$ and the density is $\rho_{ox} = 3.01\ g/cm^3$.[17]

The average fits reported for 95°C and the corresponding predictions for metal loss and dense boehmite film thickness for the USH, assuming 5 years (1825 days) in-core exposure, are in Table 5. As for the MURR, note that the USH would have been exposed to forced coolant flow rather than the minimal flow of the Draley tests.

Table 5 Literature model parameter values from reference [18] and calculated boehmite thickness for the USH.

	a (mg/dm^2)	b (mg/dm^2)	$L(1825\ days)$ (mg/dm^2)	$x_{ox}(1825\ days)$ (μm)
O_2-sat.	7.83	5.72	31.3	2.3
He-sat.	5.66	11.17	29.6	2.2

Pawel et al. [19] performed corrosion experiments on Al-6061 in a test loop with forced water flow at 9–28 m/s, pH of 4.5–5.0, heat flux of 5–20 MW/m^2, calculated water-oxide interface temperatures of 95–208°C, and durations of up to 35 days. They fitted a correlation in the form of a power law given by

$$x_{ox} = \left(x_0^{1/0.74} + \frac{1}{0.74}\ kt\right)^{0.74}$$

where x_0 is the initial film thickness at $t = 0$. The rate constant k was fitted as a function of the water-oxide interface temperature, $T_{x/c}$, and the heat flux ϕ, given by [19]

$$k = \left(6.3887 \times 10^7\ \frac{\mu m^{1.351}}{h}\right) \exp\left(\frac{-9154\ K}{T_{x/c} + (1.056\ K\ m^2/MW)\phi}\right).$$

For USH, assuming 5 years (43800 hours) exposure at a temperature of about 90°C (363 K) with no pre-existing film and negligible heat flux, this correlation predicts a rate constant of $k = 7.1 \times 10^{-4} \mu m^{1.351}/h$ and an oxide thickness $x_{ox}(43800\ h) = 16\ \mu m$.

2.6.3 Predictions for Mark-16B oxide thickness based on exposure history

Neumann [20, 21] conducted in-reactor corrosion testing on aluminum coupons of multiple alloys in the Oak Ridge Research Reactor (ORR). The ORR operated in 4-week cycles: 3 weeks of operation followed by ~1 week of downtime. Corrosion specimens were removed after various numbers of cycles. The water flowrate over the specimen holders in the core was estimated to be 8 to 12 ft/s. At power, the core inlet and outlet temperatures were 124°F (51°C) and 132°F (56°C), respectively (somewhat higher than the estimated operating temperature of ~38°C for the Mark-16B cropping). The pH of the water was usually in the range 5.5–6.5 [21].

The coupons were weighed before exposure, after removal from the core, and after chemical defilming. Only the weight losses after defilming were reported in Refs. [20, 21]. The authors reported incomplete defilming of some samples for unknown reasons, which tends to reduce the measured weight loss of the metal, in some cases resulting in a measured weight gain between the original coupon and the "defilmed" coupon. The coupons were twice dried at 120°C for an unspecified duration after cleaning, once during sample preparation (prior to the pre-exposure weighing), and again after defilming (before post-defilming weighing).

After 500 hours of exposure (21 days, at power), the two of four 6061 samples characterized showed no detectible weight loss, and the other two weight losses of 0.9 and 1.0 mg/cm^2 [20]. Assuming a dense, completely adherent oxide layer, this would correspond to about 10–12 µm of bayerite or gibbsite. After 4032 hours (168 days = 24 weeks) of exposure, 2318 hours (97 days) at power, the measured weight loss for four samples ranged from zero to 1.2 mg/cm^2 with an average of 0.4 mg/cm^2 [20]. The estimated dense film thickness would then range from about 0–14 µm of bayerite or gibbsite with an average of about 5 µm. Since the Mark-16B elements were estimated to have been in-core about 7 months (about 32 weeks), a linear extrapolation from 0 to the latter exposure times (24-week data only), for a dense oxide, would range in thickness from 0-19 µm with an average of ~7 µm. This extrapolation may be unreasonable and is for ball-parking the expected oxide thickness only; a better approach may be to just use the 24-week data for comparison.

It was not possible to delineate the oxides formed during reactor exposure from those formed in post-discharge cooling or long-term L-Basin storage. It is likely that the oxides were predominantly formed in-core, because the oxides formed at higher temperatures are generally more protective to the underlying aluminum substrate. In-core temperatures ranged from between ~40 °C and ~100 °C vs L-Basin's average of 22°C.

3.0 Oxyhydroxide Characterization and Analysis

3.1 Sample Preparation

Once at SRNL, the MURR piece was removed from the water in the cask and placed in a closed Ziploc bag in the shielded cells until the bolts were cut off using a Dremel on about 11/02/2018. It was then double-bagged and taped shut for transport out of the shielded cells. Cutting the stainless steel bolts from the cropping reduced the dose associated with the cropping and allowed for transfer of the MURR piece out of the shielded cells and into a radiological hood. In the radiological hood, an attempt was made to further decontaminate the cropping on ~11/08/2018 by scrubbing with a soft bristle brush, prior to cutting samples

using a slow-speed abrasive saw. The MURR cropping, with the section removed for XRD and SEM marked, is shown in Figure 3, middle and right.

To make the MURR samples from the MURR cropping, a section on the side of the cropping was cut along the red dotted line shown in Figure 3 (right), using a slow speed abrasive saw. This piece was then further cut into 4 pieces using the same method, with one piece sent for XRD, one for plan-view SEM, one for cross-sectional mounting for SEM, and one as a spare. The surface of the cut plate that was facing the inside of the element, with a slotted edge, was investigated by XRD and SEM plan-view. This inside surface was chosen for examination due to the disturbance of the other surfaces by the decontamination attempt (the brush used for decontamination could not reach the inside surface). XRD of the MURR cropping was completed on 12/06/2018 and SEM/ energy dispersive spectroscopy (EDS) plan-view on 12/19/2018 (first pass). SEM/EDS plan-view was repeated on 01/09/2019.

Once at SRNL, the Mark-16b and USH croppings were removed from the cask and allowed to drip dry for several hours on 8/29/2018. Then the Mark-16b and USH croppings were double bagged and J-sealed and stored until 12/10/2018, when the bag was opened, and samples were cut and sent for analysis. Figure 6 and Figure 7 show the regions of the USH and Mark-16B croppings, respectively, where the samples were cut for analysis. To make the USH samples from the USH cropping, straight-cut aviation snips were used to cut a roughly square piece from the edge, which was cut into smaller pieces, with the grid for the samples shown in Figure 6, and dispositioned like the MURR pieces. To make the Mark-16B samples from the Mark-16B cropping, large bolt cutters were used to cut 5 pieces from the water inlet shown in Figure 7 and dispositioned like the MURR pieces, except the extra piece was also kept as a spare. XRD for both USH and Mark-16B was completed 12/13/2018, and SEM/EDS plan-view was completed on 01/09/2019.

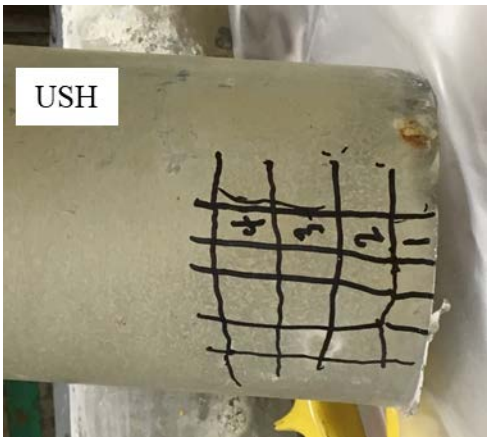

Figure 6 USH cropping marked for cutting of samples

Figure 7 Mark-16B cropping marked for cutting of samples.

The cropping samples meant for cross-sectional viewing in the contained SEM were mounted together in EpoFix. Glass slides were placed between samples in the epoxy mount to reduce pressure on the samples during grinding and polishing.

The EDS results should be interpreted with caution. In general, EDS spatial resolution can often be assumed to range from a micron to several microns in diameter on the sample surface and into the sample.[22] More accurately, the spatial resolution is a function of the sample chemistry, density, and SEM accelerating beam voltage.[23] Using the Anderson and Hasler model for x-ray generation range, the spatial resolution for Al and O in a material with a density of 2.7 g/cm^3 (aluminum) is about 3.6 µm, but the spatial resolution for Al and O in a material with a density of 4 g/cm^3 (Al_2O_3) is about 2.5 µm.[23]

3.2 XRD Analysis

X-ray diffraction was performed on pieces from the 3 croppings. The resulting spectra for the MURR, USH, and Mark-16B croppings are shown in Figure 8, Figure 9, and Figure 10, respectively.

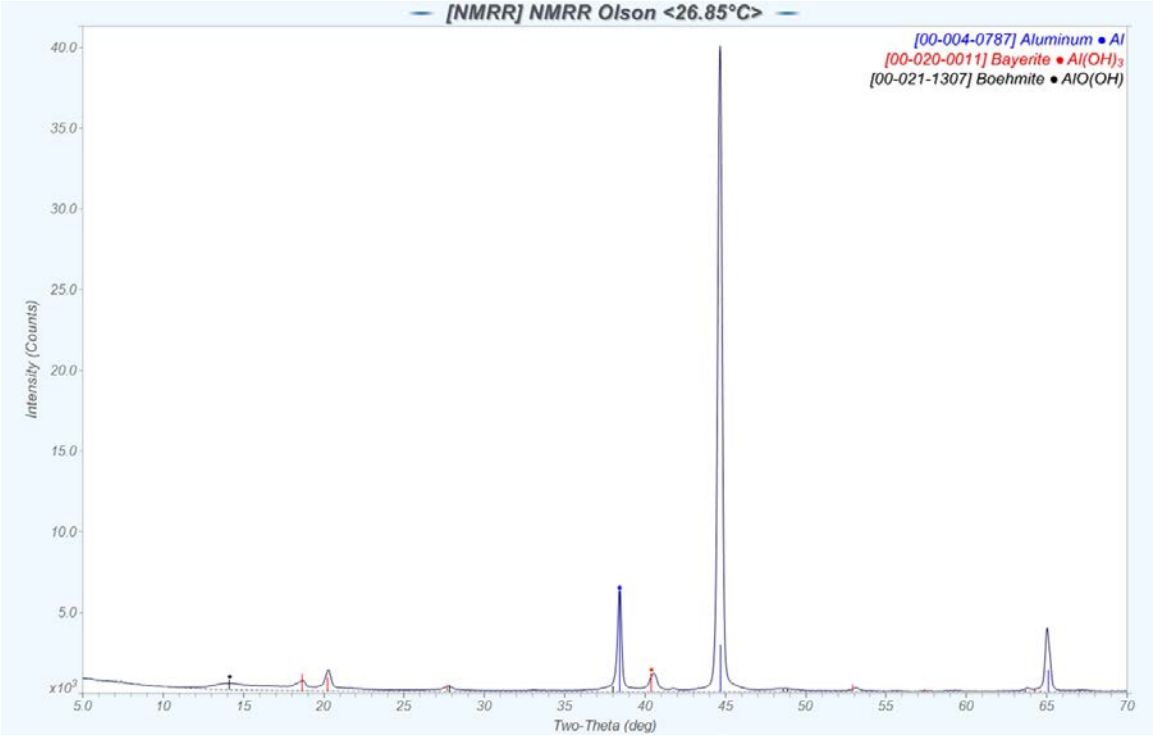

Figure 8 XRD spectrum of MURR cropping oxide.

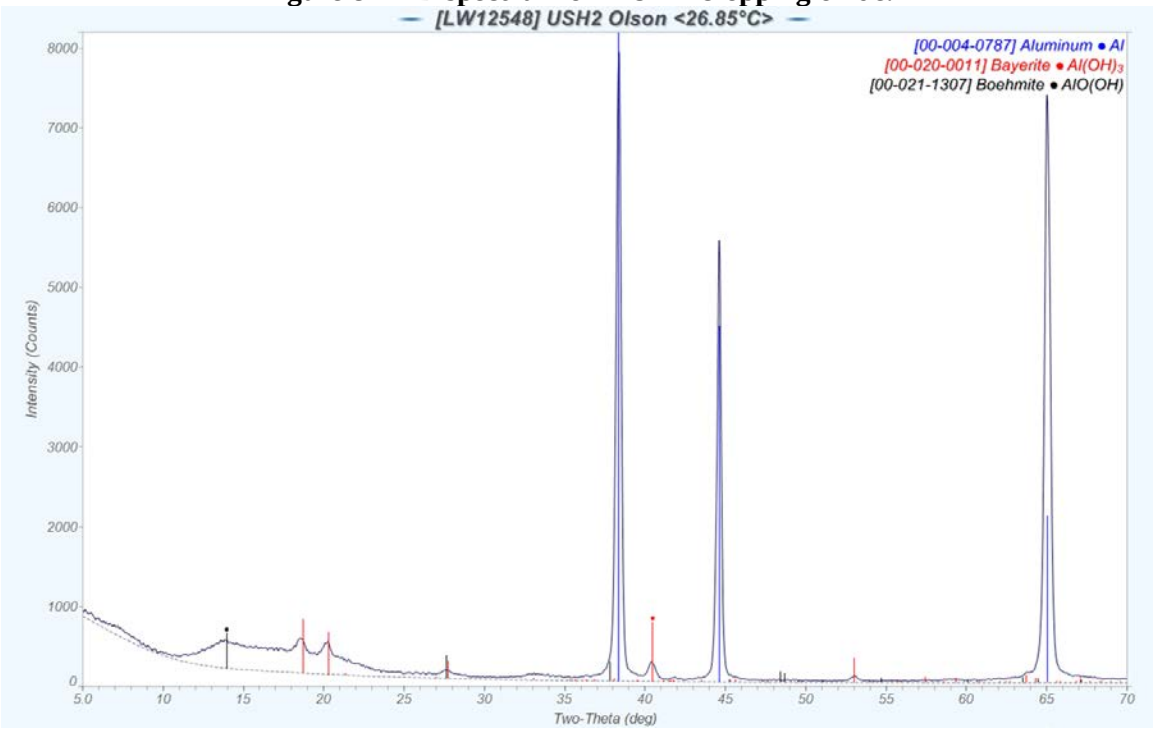

Figure 9 XRD spectrum of USH cropping oxide.

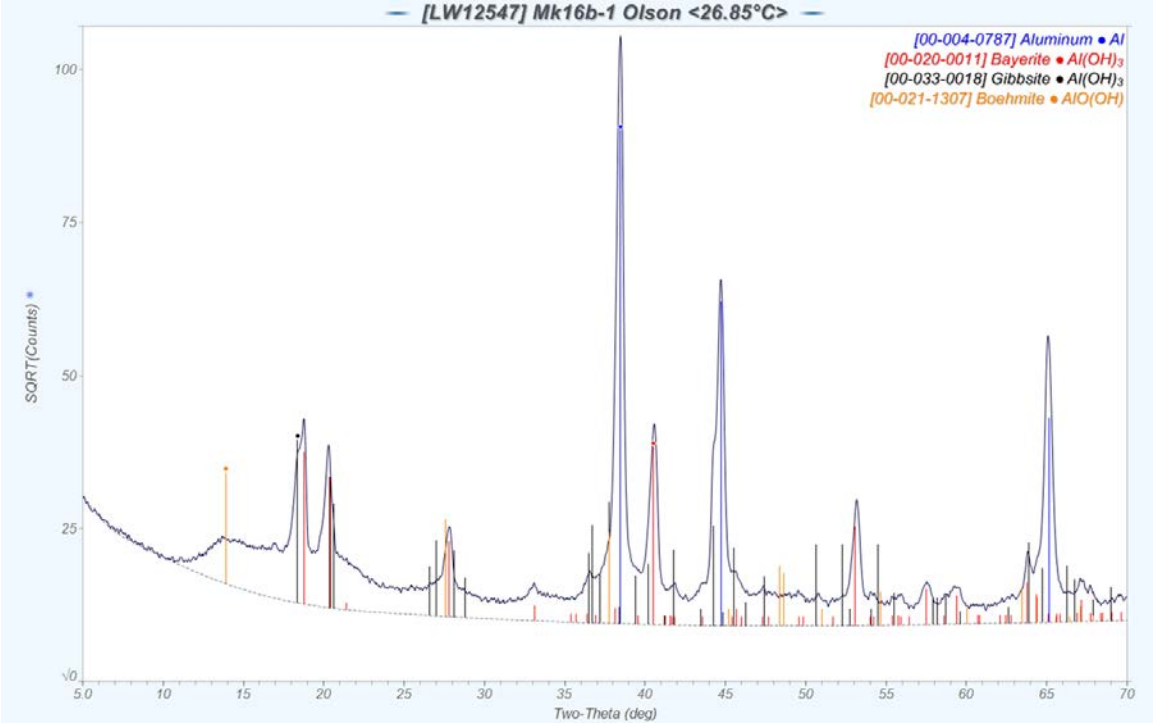

Figure 10 XRD spectrum of Mark-16B cropping oxide.

Comparison of the XRD spectra show the oxide peaks becoming stronger in relation to the base aluminum peaks, moving from the MURR, to the USH, and then the Mark-16B, implying progressively thicker oxides. Similar visual observations were made during sample cutting. All the samples have bayerite and boehmite present, with just the Mark-16B, believed to have operated in the coldest environment, having gibbsite. Comparison of the strength of the oxide peaks shows the boehmite signal relative to the bayerite signal was a larger ratio for the USH compared to the other two samples. The scale-adjusted spectra in Figure 11 show in more detail the larger relative boehmite peak to bayerite peak in the USH sample (middle), followed by the MURR, with the oxide peaks in the Mark-16B being dominated by the bayerite. Trihydroxides, such as gibbsite, form at temperatures below ~80 °C.[24] Based on the comparison of the oxide peaks, known operation histories, length of time in wet storage, and assuming oxide formation in the storage pool has not dominated the oxide formation on the samples, it can be surmised that the USH was exposed to the highest, boehmite-forming temperatures, followed by the MURR, and lastly the Mark-16B which had the lowest temperature exposure.

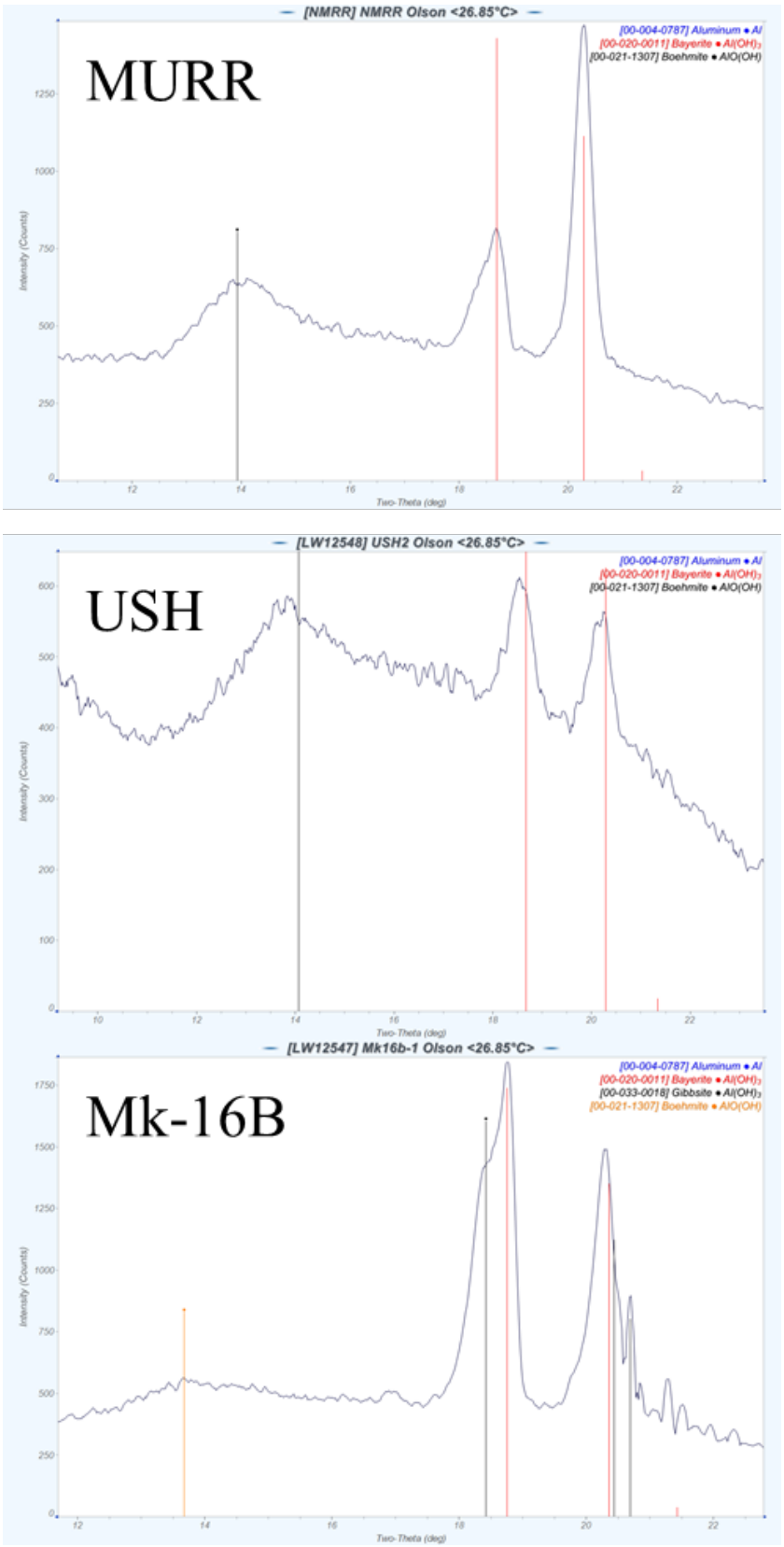

Figure 11 Narrowed x-axis window of 2theta to 8-23 degrees and y-axis decreased.

The extent to which the presence of boehmite impacts the growth of gibbsite and bayerite is unknown and may complicate the growth and relative ratios of oxides. Characterization of surrogate oxides grown without boehmite, on Al-1100 using a hot-wall immersion method at 50 °C [25] identified the oxide as bayerite, a trihydroxide polymorph. Oxides grown on Al-6061 under similar conditions [26] were also identified as predominantly bayerite, possibly accompanied by a smaller amount of gibbsite. The specific trihydroxide polymorphs formed for corrosion below ~80 °C have been found to depend on environmental characteristics such as pH and/or presence of impurities in the water, with bayerite formation associated with the absence of impurities and near-neutral pH (~5.8 to ~9) while gibbsite was associated with the presence of impurities (such as solutions of NaOH or KOH) or high (>9) or low (<5.8) pH [17, 24].

3.3 MURR SEM Plan-View

Oxides were found that appear to have remained intact from wet storage and unaffected by decontamination attempts. Oxides on MURR appear to be blocky and dense, Figure 12, like that observed on a dry-stored RU-1 sample and reported in SRNL-STI-2018-00428.[27]

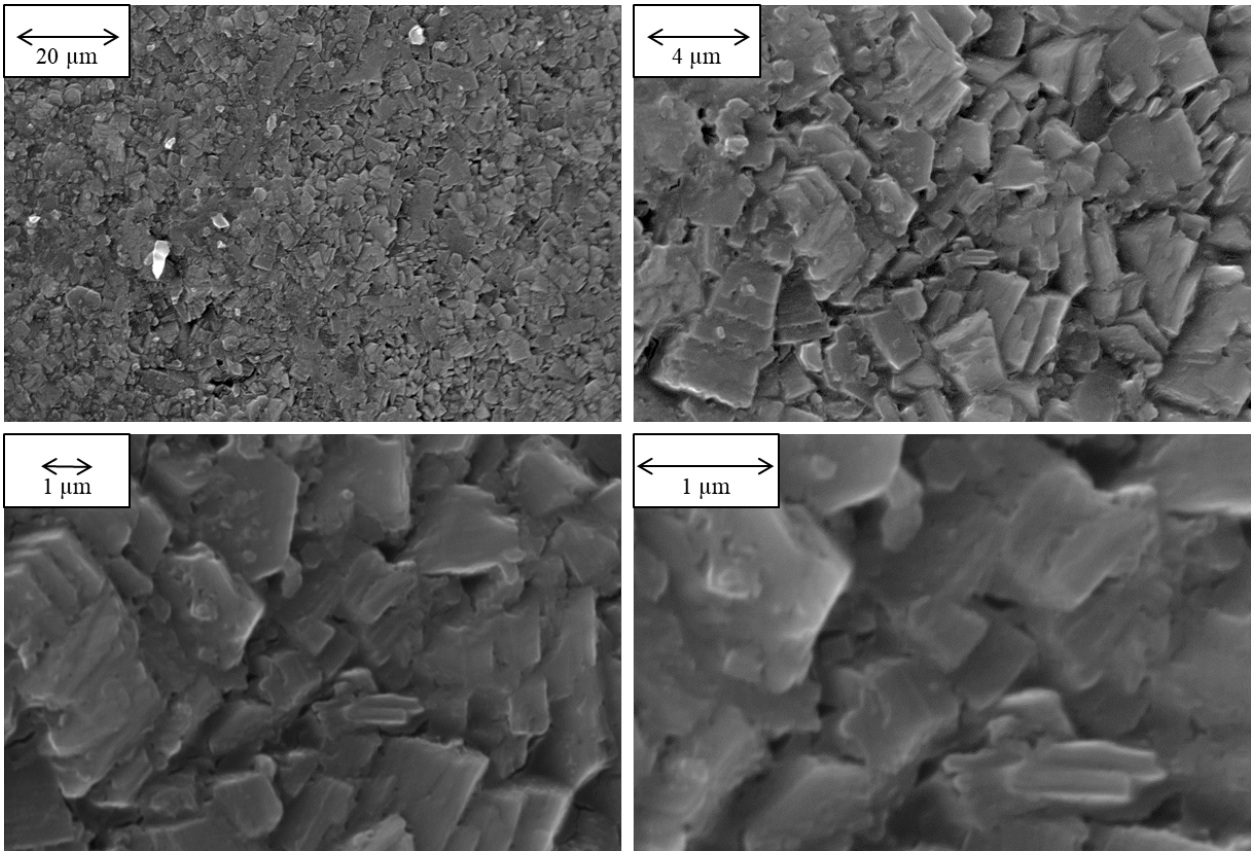

Figure 12 SEM Plan-view of MURR oxide

3.4 MURR SEM Cross-section

The MURR sample cross-section is shown in Figure 13, with EDS line-scan in Figure 14. The oxide on the inside stepped edge, which would have been between the grooves holding the fuel plates, was ~5-10 µm thick. The oxide was relatively uniform in thickness over the region examined, staying mostly near ~10 µm in thickness.

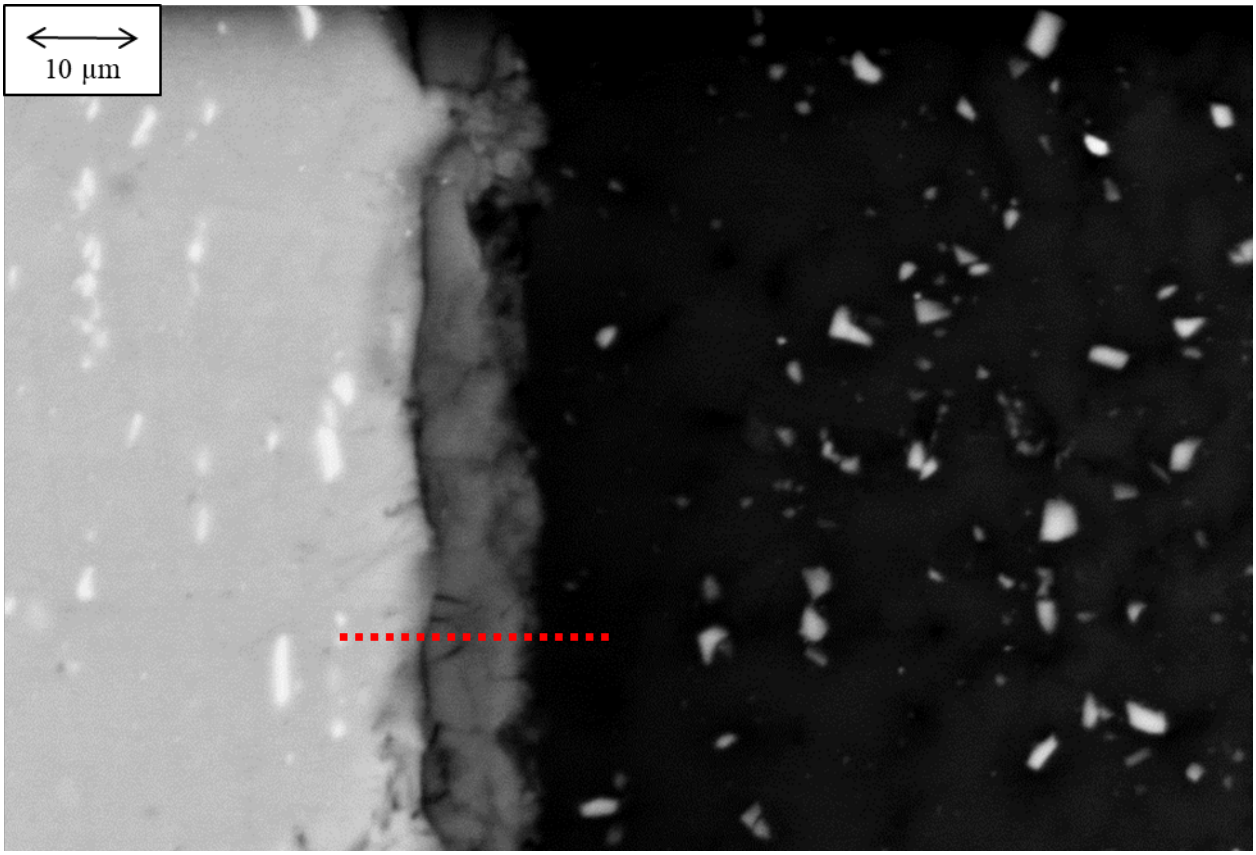

Figure 13 SEM of MURR cross-section showing oxide layer thickness.

The EDS line scan in Figure 14 shows the oxygen-enriched passivation layer, and a gradual decrease in the aluminum concentration as the EDS measurements are taken progressively closer to the mount. The carbon from the mount as well as from contamination influences the relative amount of aluminum and oxygen detected, so the ratio of oxygen to aluminum may not be a good metric to determine the oxide polymorph.

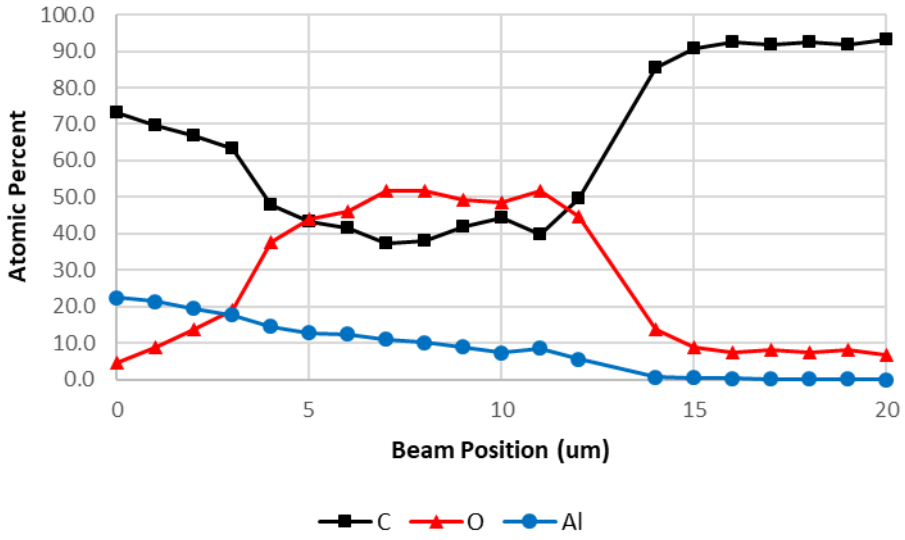

Figure 14 EDS line scan corresponding to dashed red line in Figure 13. EDS results have been normalized to show exclusively carbon (which is present in the mounting material and as surface contamination), Al, and O.

3.5 USH SEM Plan-View

Oxides on USH appear to be blocky and dense, Figure 15, and denser and smoother than on the MURR sample.

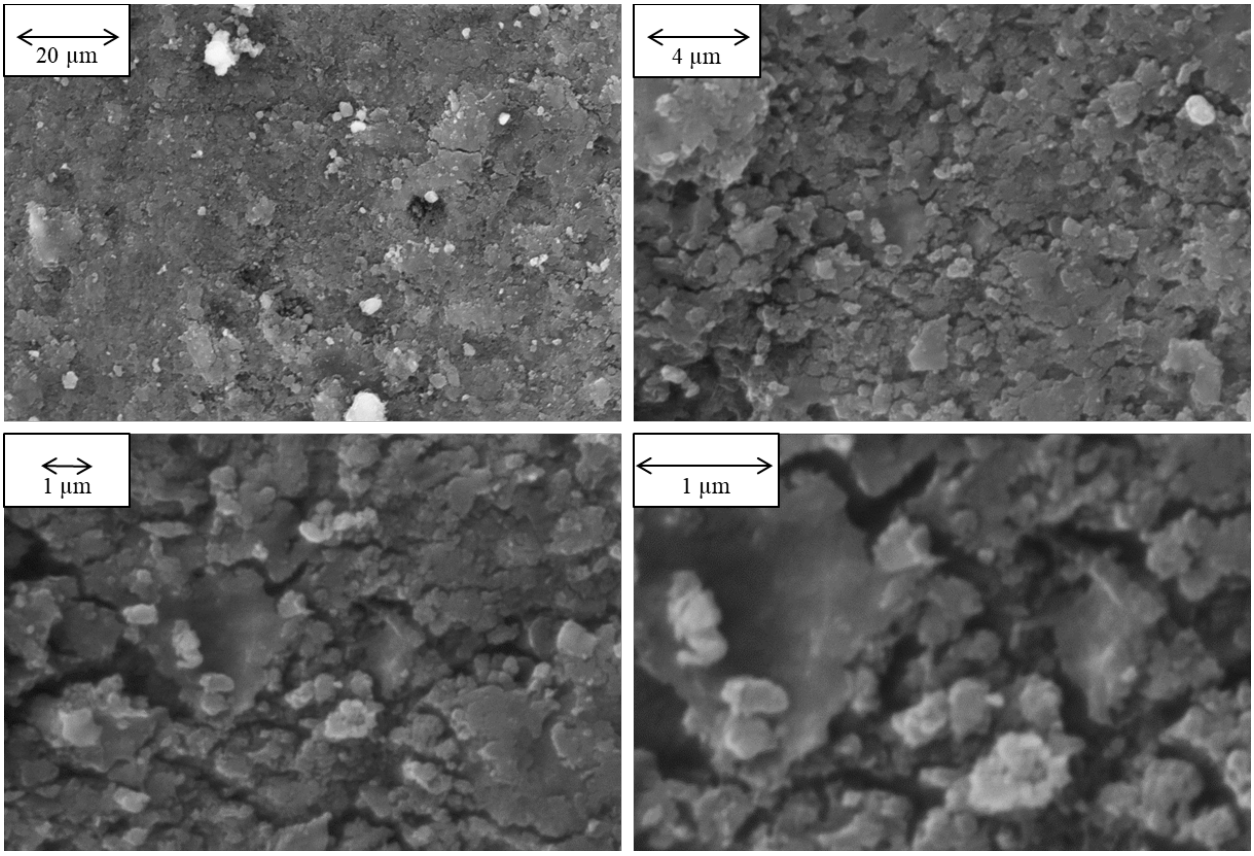

Figure 15 SEM plan-view of the surface of a USH cropping

3.6 USH SEM Cross-section

The USH sample cross-section is shown in Figure 16, with EDS line-scan in Figure 17. The SEM and EDS cross-section results could not indicate a discernible oxide. The lack of a discernible oxide indicates that it was either thin or did not survive the sample preparation. Due to oxides surviving on the MURR and Mark-16B samples, oxide being visible in the plan-view USH sample, and XRD indicating that the sample oxide was mostly boehmite (an oxide that develops very slowly), it is believed that the oxide is present, but very thin (<1 µm) since it is not clearly visible in Figure 16. It is possible a technique that can provide better contrast and edge retention may allow for imaging of the thin oxide layer if present, such as Ni plating. The EDS line scan in Figure 17 has a small bump that may correspond to the oxide layer, but it is not overtly clear. There is also a gradual decrease in the aluminum concentration as the EDS measurements are taken progressively closer to the mount. The carbon from the mount as well as advantageous carbon influences the relative amount of aluminum and oxygen detected, so the ratio of oxygen to aluminum may not be a good metric to determine the oxide polymorph.

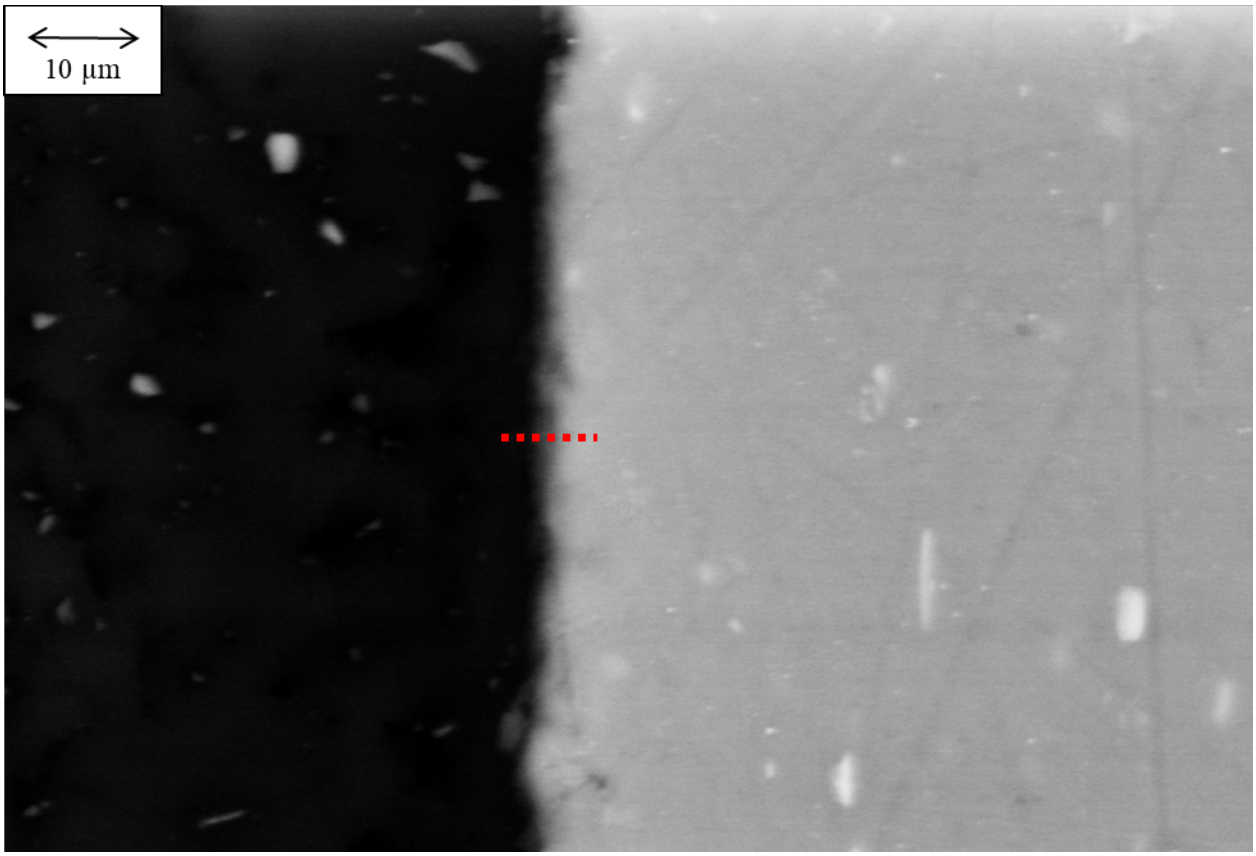

Figure 16 SEM of USH cross-section showing lack of visible oxide layer.

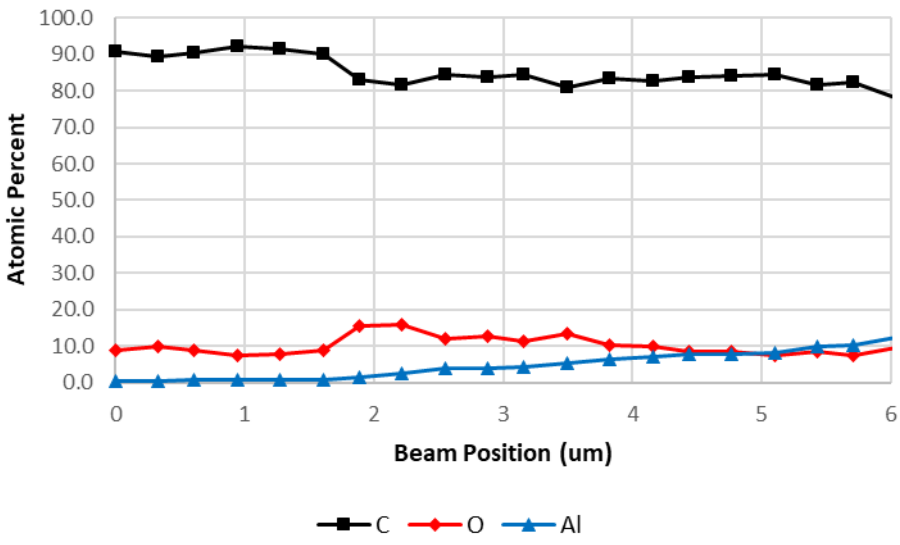

Figure 17 EDS line scan corresponding to dashed red line in Figure 16. EDS results have been normalized to show exclusively carbon (which is present in the mounting material and as surface contamination), Al, and O.

3.7 Mark-16B SEM Plan-View

The oxide on the Mark-16B sample was found to have spalled off near an edge, assumed to been caused by the cutting operation utilizing a bolt-cutter, Figure 18. This provided an opportunity to examine the surface beneath the thick oxide, hypothesized to have a thinner oxide coating due to EDS results (discussed in section 3.9). The thick oxide coating was also examined.

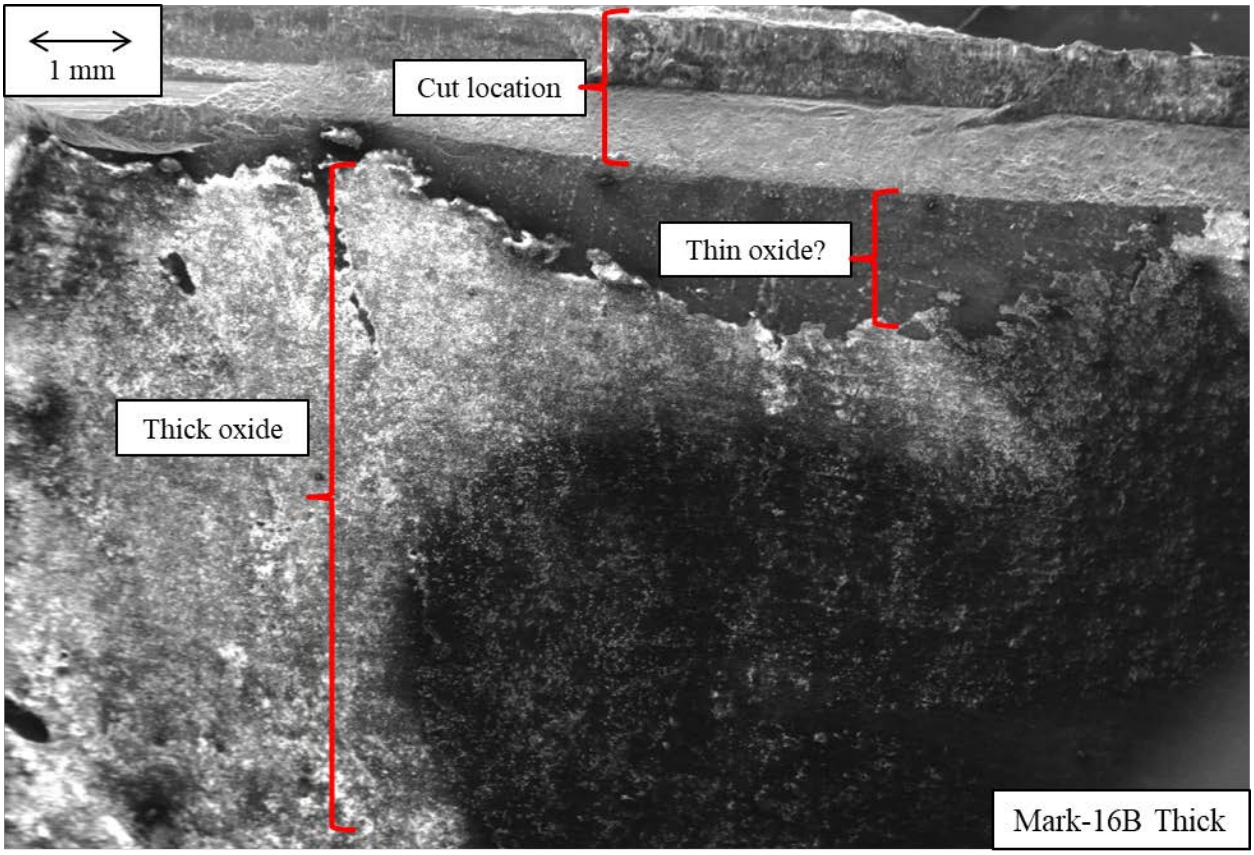

Figure 18 Top: SEM showing region of Mark-16B sample near cut edge with broken oxide. Bottom left: Thick oxide region. Bottom right: spalled oxide region.

Figure 19 shows the spalled oxide region. The oxide, if present, appears to be nodule-like, with sporadic pits, but in general dense, in contrast to the thick oxide images.

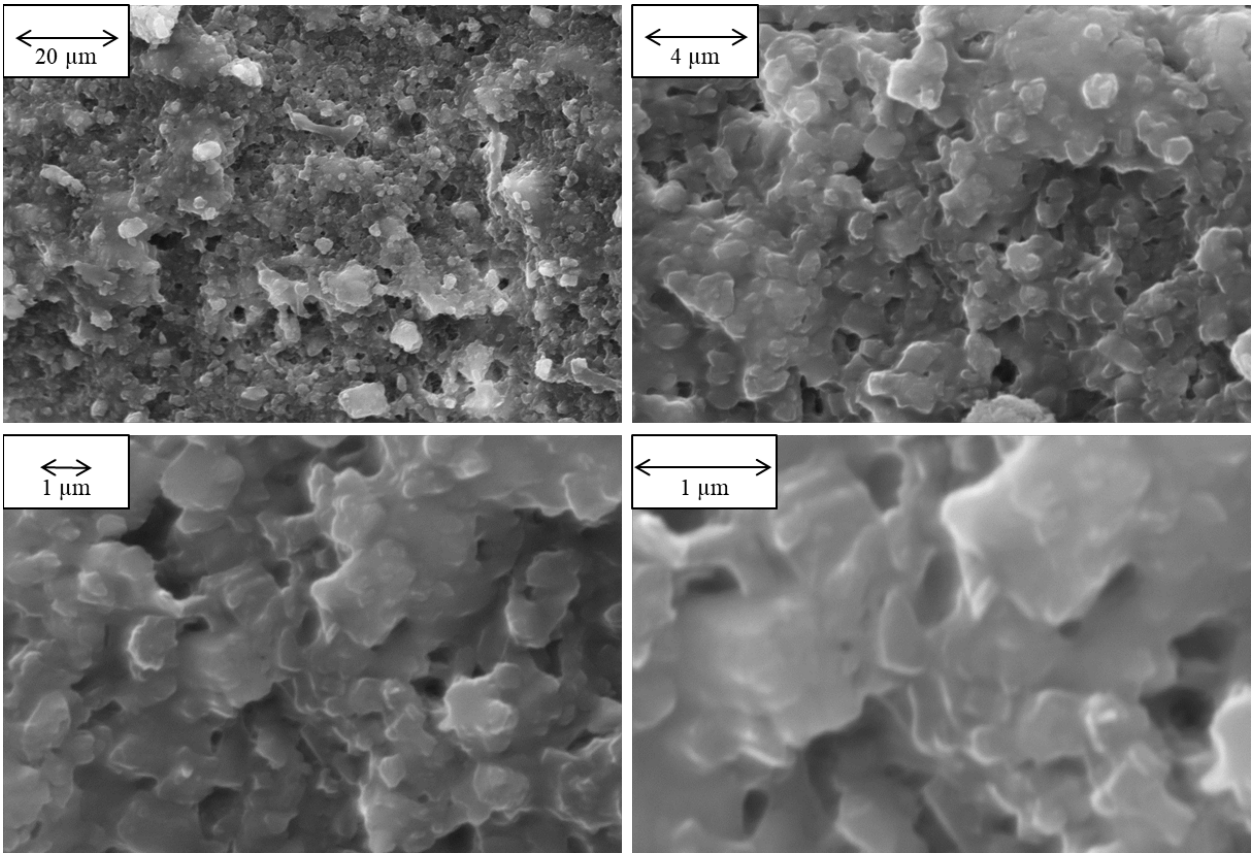

Figure 19 Spalled oxide region on Mark-16B sample.

Figure 20 shows the thick oxide. The oxide appears to be blocky in shape, but with a highly irregular surface resulting in a porous structure.

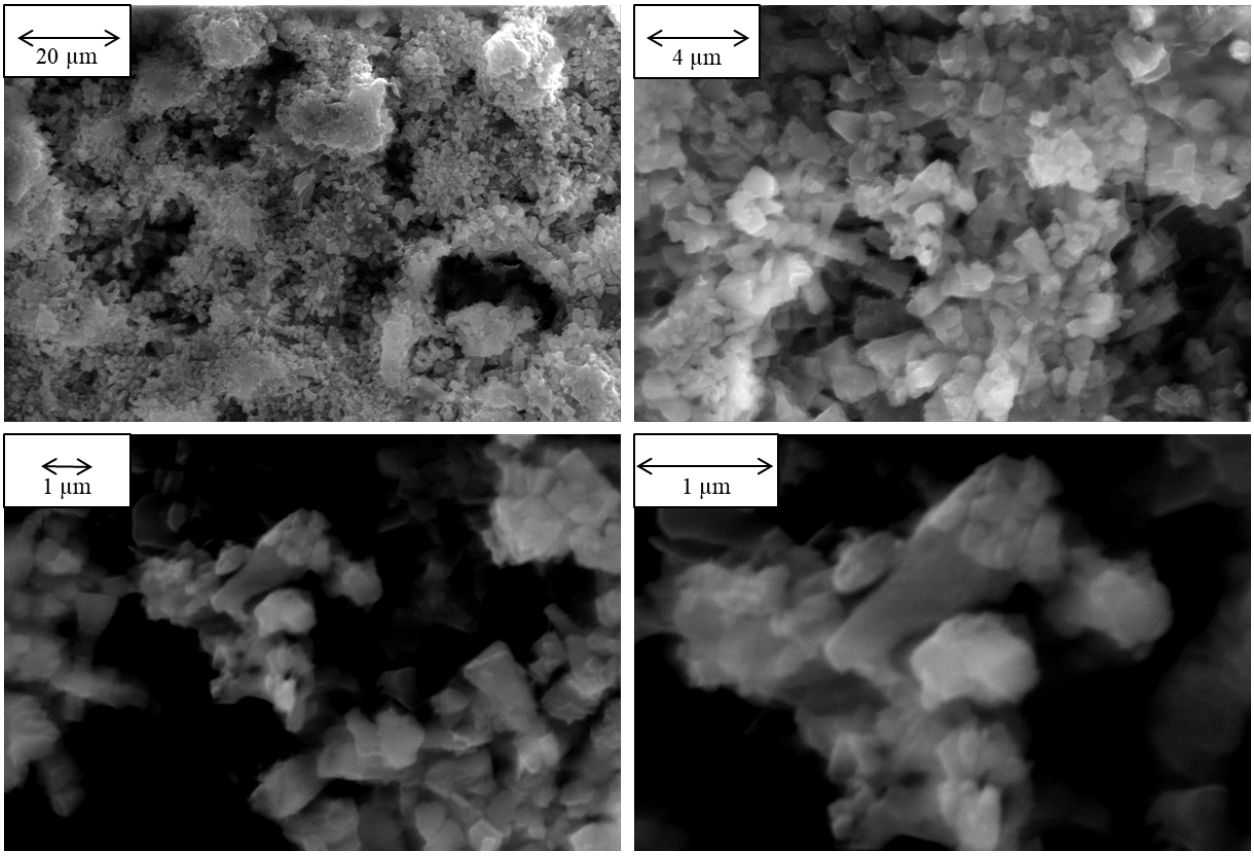

Figure 20 Thick oxide region of the Mark-16B sample

3.8 Mark-16B SEM Cross-section

The Mark-16B sample cross-section is shown in Figure 21, with EDS line-scan in Figure 22. The oxide was relatively uniform over the surface cross-section examined and varied from ~5 to ~15 µm in thickness, but on average appeared to be about 10 µm. The EDS line scan in Figure 22 shows the oxide enriched passivation layer and a gradual decrease in the aluminum concentration as the EDS measurements are taken progressively closer to the mount. The carbon from the mount as well as advantageous carbon influences the relative amount of aluminum and oxygen detected, so the ratio of oxygen to aluminum may not be a good metric to determine the oxide polymorph.

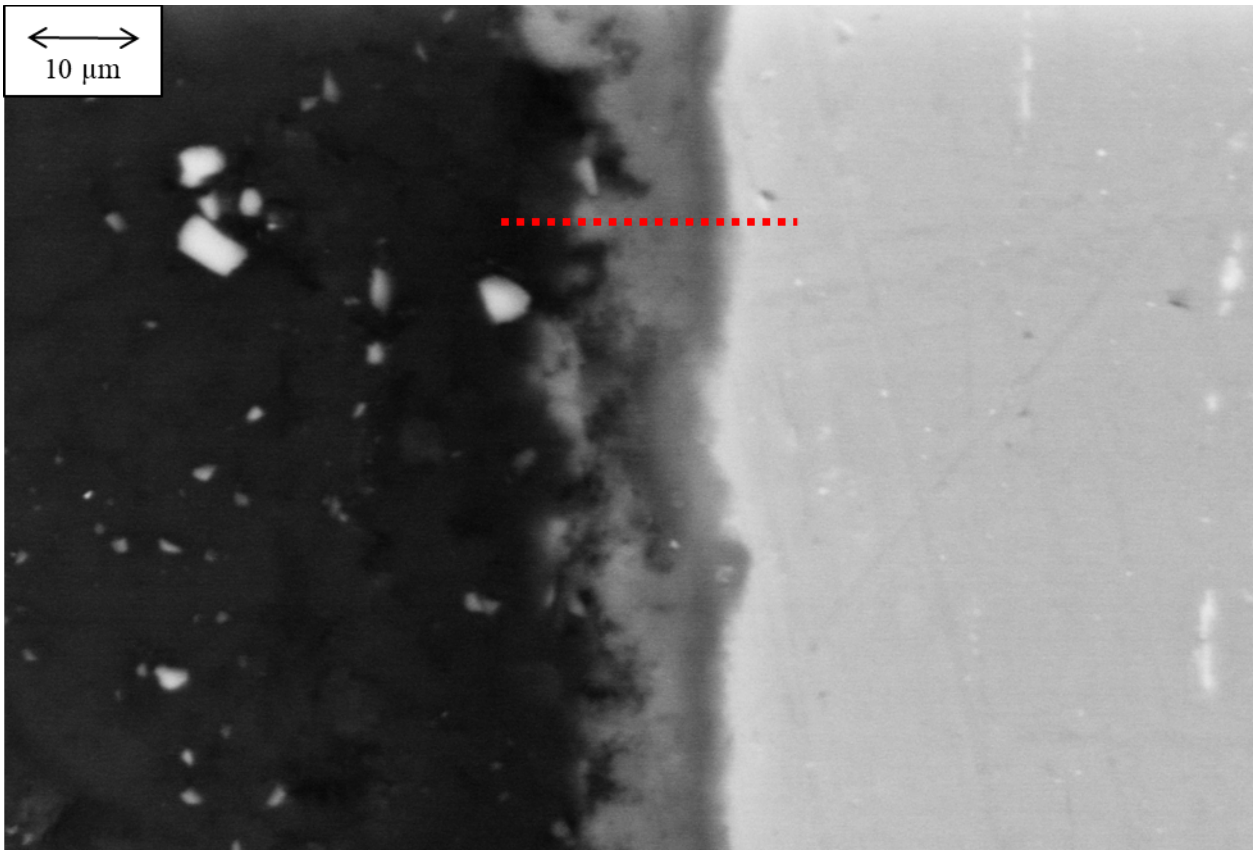

Figure 21 Mark-16B SEM of cross-section showing oxide layer thickness.

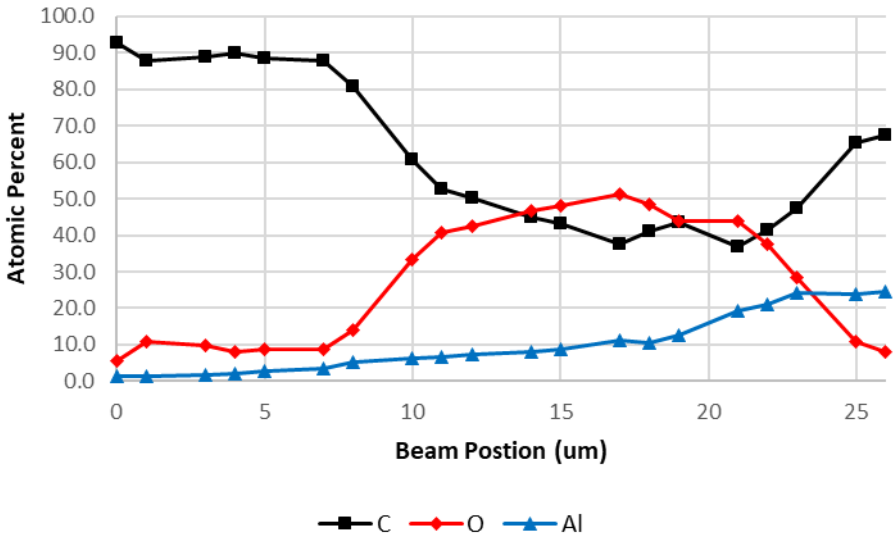

Figure 22 EDS line scan corresponding to dashed red line in Figure 21. EDS results have been normalized to show exclusively carbon (which is present in the mounting material and as surface contamination), Al, and O.

3.9 Plan-View EDS Comparison

EDS of the plan-view oxides was performed to provide verification of oxide presence and an indication of thickness. Figure 23 shows the region of the EDS raster scans of the oxide surfaces, with the results shown in Table 6. Because the oxide thickness is unknown, and the EDS active region could extend through the oxide and into the aluminum base alloys, caution is warranted interpreting the EDS data. The molecular atomic percent for the oxygen component (based on the aluminum oxide polymorph chemical formula), should be 50% for pure, thick boehmite, AlO(OH), 43% for gibbsite and bayerite, $Al(OH)_3$, and 60% for alumina, Al_2O_3. However, because EDS cannot detect hydrogen, we should expect to see atomic percentages of O to Al of 67% O for boehmite, and 75% O for gibbsite and bayerite, when examined by EDS. Alumina forms in air at room temperature but is not stable in water until temperatures exceed 360°C.[17] The USH EDS is either indicative of boehmite, or the EDS probe is picking up the underlying alloy. The EDS on the thick Mark-16B and the MURR appears indicative of bayerite/gibbsite. The thin oxide Mark-16B spectra appears to have a contribution from aluminum substrate.

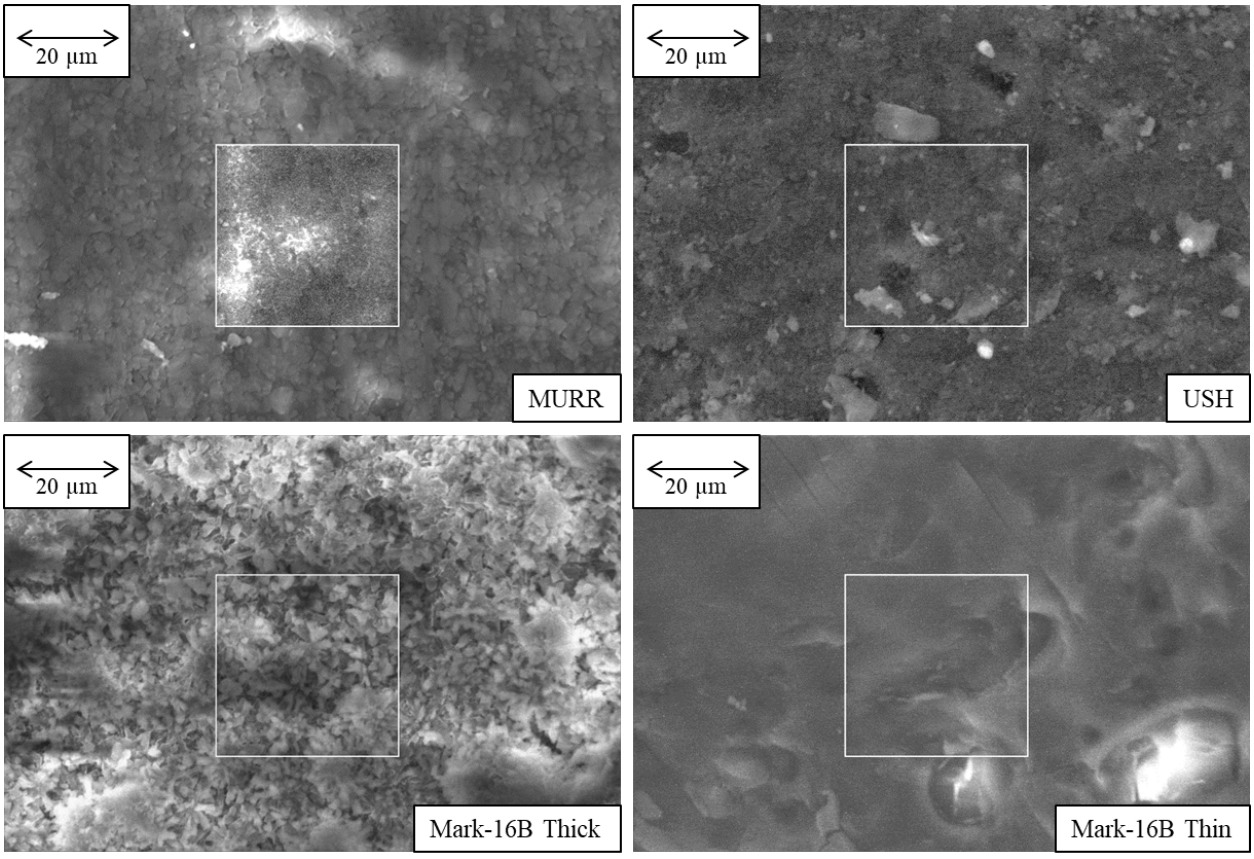

Figure 23 SEM with boxes marking the regions of the EDS area scan.

Table 6 EDS area scan data corresponding to regions in Figure 23.

All results in atomic%							
Spectrum	O	Mg	Al	Si	S	Fe	Zn
Thick oxide Mk16B	79.8		20.1	0.2		0.0	
Thin oxide Mk16B	46.1	0.5	51.2	2.2		0.1	
USH	63.4	0.1	35.7	0.7	0.1	0.1	0.1
MURR	77.6	0.0	22.3			0.1	
All results in atomic% (O_2 and Al only, data renormalized)							
Spectrum	O	Mg	Al	Si	S	Fe	Zn
Thick oxide Mk16B	79.9	-	20.1	-	-	-	-
Thin oxide Mk16B	47.4	-	52.6	-	-	-	-
USH	64.0	-	36.0	-	-	-	-
MURR	77.7	-	22.3	-	-	-	-

Figure 24 shows the four measurements EDS spectrums for the oxide peak (first peak on left) compared to the aluminum substrate peak (right), showing in a more graphical format the relative strength of the oxygen and aluminum signals.

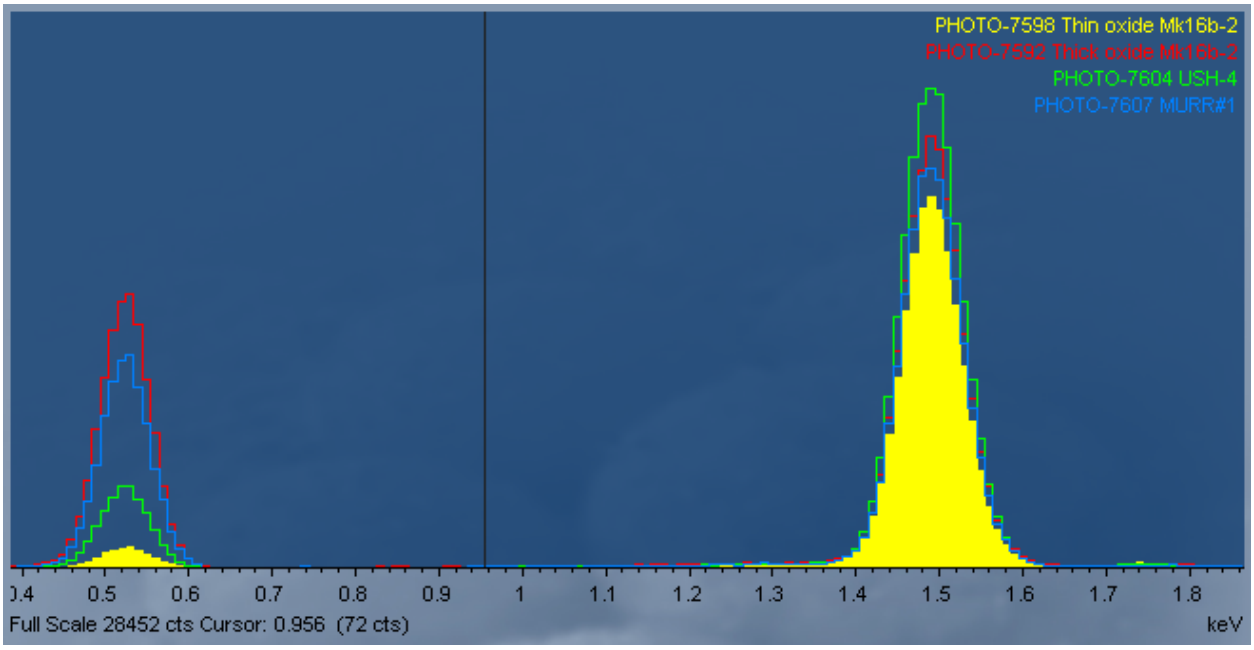

Figure 24 Comparison of the EDS spectra corresponding to Figure 23.

4.0 Summary of Results

Oxyhydroxides were characterized from the cladding surface on one cropped piece of 6061, one cropped piece of 6063, and one cropped piece of either 6061 or 6063 cropping, stored wet for up to 50 years in L-Basin on the Savannah River Site. SEM, EDS, and XRD were performed on pieces cut from the croppings to evaluate the composition and morphology of oxides on the cladding surface. Observations and results are provided below:

- The presence of oxides was identified with XRD and confirmed via EDS on all 3 L-Basin wet stored samples.
- Predicted values to characterized values of oxide thickness are shown in Table 7.

Table 7 Oxide thickness summary and comparison to values derived from literature

Sample	Predicted range* (µm)	Observed Range (µm)
MURR	4-5	5-10
USH	2-16	ND
Mark-16B	0-19	5-15

*Origin of predicted values are discussed in section 2.6. Some predicted values are tenuous extrapolations and are given for ball-parking purposes only.
ND: Not detected in cross-section in SEM

- XRD analysis revealed bayerite, $Al(OH)_3$, and boehmite, AlO(OH), on the surface of the MURR and USH samples, and bayerite, boehmite, and gibbsite, $Al(OH)_3$, on the surface of the Mark-16B sample. The presence of the bayerite on the USH, which is believed to have operated at close to 90°C, suggest that further oxide growth in wet storage will need to be accounted for, despite the apparent protectiveness of the 185°C prefilms.
- The XRD peak comparison of boehmite to bayerite indicates the USH had the highest exposure temperatures with the most boehmite being formed, followed by the MURR. The Mark-16B had the least boehmite detected. Review of historical literature supports these conclusions.
- The surface oxide morphology from plan-view of the MURR sample appears blocky and dense, which is expected to be more protective than a porous film.
- The surface oxide morphology from plan-view of the USH appeared globular and dense, which is expected to be more protective than a porous film.
- The surface oxide morphology from plan-view of the Mark-16B primary oxide appeared blocky but porous. Where the thick oxide fractured off near the edges of the sample from cutting, it appeared a uniform thin oxide was present.

5.0 References

[1] C. Verst, "RE: L-Basin milestone data packet," R. S. Luke Olson , David Herman, Roderick Fuentes, Anna d'Entremont, Ed., Probable L-basin exposure temeprature and times ed. SRNL, 2018.

[2] J. P. Howell, "Corrosion Surveillance In Spent Fuel Storage Pools," presented at the Corrosion97, New Orleans, Louisiana, 1997.

[3] R. Butler, et. al., "License Renewal Application Safety Analysis Report: Missouri University Research Reactor (MURR)," August 18 2006.

[4] J. Stillman, Feldman, E., Foyto, L., Kutikkad, K., McKibben, J.C., Peters, N., Stevens, J. , "Technical Basis in Support of the Conversion of the University of Missouri Research Reactor (MURR) Core from Highly-Enriched to Low-Enriched Uranium – Core Neutron Physics, Argonne National Laboratory technical document, ANL/RERTR/TM-12-30," September 2012.

[5] J. Stillman, Feldman, E., Foyto, L., Kutikkad, K., McKibben, J.C., Peters, N., Stevens, J. , "Conceptual Design Parameters for MURR LEU U-Mo Fuel Conversion Design Demonstration Experiment, Argonne National Laboratory report: ANL/RERTR/TM-12-38 Revision 1," March 2013.

[6] L. Foyto, "RE: Fuel storage pool pH and pool water chemistry," L. Olson, Ed., MURR Pool Water Chemistry data/trends for calendar year 2018 ed. SRNL, 2019.

[7] C. Verst, "Re: Items for wet stored L-Basin scrap final report," L. Olson, Ed., ed. SRNL, 2019.
[8] J. P. Howell, Zapp, P.E., Nelson, D.Z., "Corrossion of aluminum alloys in a reactor disassembly basin (U), Westinghouse Savannah River Company technical document, WSRC-MS-92-393," 1992.
[9] K. E. Metzger, "Task Technical and Quality Assurance Plan for Aluminum Clad SNF Dry Storage Studies, Savannah RIver National Laboratory technical document, SRNL-RP-2018-00610 Revision 0," June 6 2018.
[10] C. Verst, "FW: USH and Mark-16B steam drying temperature and time," L. Olson, Ed., email describing steam drying time and temperature ed. SRNL, 2019.
[11] SRS, "SRS Production Reactor SAR, table 5.4-1 Process Water System Heat Exchanger Design Data," p. 0506/E/1, 07/17 1989.
[12] C. Verst, "RE: ush temp from HX document reference," L. Olson, Ed., USH service temperature and cropping location ed. SRNL, 2019.
[13] M. Dunsmuir, "MK 16B and USH history," C. V. Kathryn Metzger, Ed., Mark-16B and USH probable temperaures based on reactor operating data ed. SRNL, 2018.
[14] SRP, "Auxiliary Sleeve ('B' Outer Chuck), Savannah River Plant technical drawing, ST-MDX58835," May 15 1974.
[15] SRP, "Mark-16B Assembly (U), Savannah River Plant technical drawing, ST-MDX5-9147," March 30 1976.
[16] J. E. Draley, Mori, S., Loess, R. E. , "The Corrosion of 1100 Aluminum in Oxygen‐Saturated Water at 70° C," *Journal of The Electrochemical Society*, vol. 110, pp. 622-627, 1963.
[17] K. Wefers and C. Misra, "Oxides and hydroxides of aluminum," Alcoa Laboratories Pittsburgh, PA Alcoa Technical Paper #19, 1987.
[18] J. E. Draley, S. Mori, and R. E. Loess, "The Corrosion of 1100 Aluminum in Water from 50° to 95° C," *Journal of The Electrochemical Society*, vol. 114, pp. 353-354, 1967.
[19] S. J. Pawel, D. K. Felde, and R. E. Pawel, "Influence of coolant pH on corrosion of 6061 aluminum under reactor heat transfer conditions," Oak Ridge National Lab.1995.
[20] P. Neumann, "Corrosion in the Oak Ridge research reactor core-cooling system," Oak Ridge National Lab., Tenn.(US)1960.
[21] P. Neumann, "The corrosion of aluminum alloys in the Oak Ridge Research Reactor," Oak Ridge National Lab., Tenn.1961.
[22] M. Dewar, "Characterization and Evaluation of Aged 20Cr32Ni1Nb Stainless Steels," Master of Science in Materials Engineering, Department of Chemical and Materials Engineering, University of Alberta, Edmonton, Alberta, 2013.
[23] J. Goldstein, Newbury, D.E., Joy, D.C., Lyman, C.E., Echlin, P., Lifshin, E., Sawyer, L., Michael, J.R., *Scanning Electron Microscopy and X-Ray Microanalysis*.
[24] B. Rabin, M. Meyer, J. Cole, I. Glagolenko, G. Hofman, W. Jones, *et al.*, "Preliminary Report on U-Mo Monolithic Fuel for Research Reactors," Idaho National Laboratory INL/EXT-17-40975, 2017.
[25] K. E. Metzger, R. Fuentes, A. d'Entremont, L. Olson, and R. Sindelar, "Preparation of aluminum oxide films under water exposure - Preliminary report on 1100 series alloys," Savannah River National Laboratory SRNL-STI-2018-00427, 2018.
[26] A. L. d'Entremont, R. E. Fuentes, L. C. Olson, and R. L. Sindelar, "Preparation of Aluminum Oxide Films Under Water Exposure – Preliminary Report on 6061 Series Alloys," Savannah River National Laboratory SRNL-STI-2018-00449, 2018.
[27] L. Olson, Fuentes, R., d'Entremont, A., Sindelar, R., "Characterization of Oxyhydroxides on a Dry-Stored Fuel Plate From L-Basin, Savannah RIver National Laboratory technical document, SRNL-STI-2018-00428, Revision 0 " October 2018.

Distribution:

SRNL:
Records Administration (EDWS)
william.bates@srnl.doe.gov
Matthew.Garrett@srnl.doe.gov
kristine.zeigler@srnl.doe.gov
Marissa.Reigel@srnl.doe.gov
Brenda.Garcia-Diaz@srnl.doe.gov
bruce.wiersma@srnl.doe.gov
anna.dentremont@srnl.doe.gov
Roderick.Fuentes@srnl.doe.gov
Luke.Olson@srnl.doe.gov
robert.sindelar@srnl.doe.gov
ps.lam@srnl.doe.gov
Christopher.verst@srnl.doe.gov
David.herman@srnl.doe.gov

INL:
michael.connolly@inl.gov
josh.jarrell@inl.gov